Hindawi Publishing Corporation
Journal of Composites
Volume 2014, Article ID 795984, 10 pages
http://dx.doi.org/10.1155/2014/795984

Research Article

High Strain Rate Compressive Behavior of Polyurethane Resin and Polyurethane/Al_2O_3 Hollow Sphere Syntactic Foams

Dung D. Luong,[1] Vasanth Chakravarthy Shunmugasamy,[1] Oliver M. Strbik III,[2] and Nikhil Gupta[1]

[1] *Department of Mechanical and Aerospace Engineering, Polytechnic School of Engineering, New York University, Brooklyn, NY 11201, USA*
[2] *Deep Springs Technology, LLC, 4750W, Bancroft Street, Toledo, OH 43615, USA*

Correspondence should be addressed to Nikhil Gupta; ngupta@nyu.edu

Received 27 July 2014; Revised 20 September 2014; Accepted 28 September 2014; Published 29 October 2014

Academic Editor: Masamichi Kawai

Polyurethane resins and foams are finding extensive applications. Seat cushions and covers in automobiles are examples of these materials. In the present work, hollow alumina particles are used as fillers in polyurethane resin to develop closed-cell syntactic foams. The fabricated syntactic foams are tested for compressive properties at quasistatic and high strain rates. Strain rate sensitivity is an important concern for automotive applications due to the possibility of crash at high speeds. Both the polyurethane resin and the syntactic foam show strain rate sensitivity in compressive strength. It is observed that the compressive strength increases with strain rate. The energy absorbed up to 10% strain in the quasistatic regime is 400% higher for the syntactic foam in comparison to that of neat resin at the same strain rate.

1. Introduction

A class of closed cell porous composites called syntactic foam is prepared by dispersing hollow filler particles in a matrix medium [1, 2]. The mechanical (compressive, tensile, and flexural) [3, 4], thermal (coefficient of thermal expansion (CTE) and thermal conductivity) [5–7], and electrical (dielectric constant) [8–10] properties of syntactic foams can be tailored based on the volume fraction and the wall thickness of the reinforcing hollow spherical filler particles. Epoxy, vinyl ester, polyester, and bismaleimide resins are examples of polymers that have been used previously in syntactic foams [2, 11]. Lightweight metals such as magnesium and aluminum are also extensively used in fabricating syntactic foams [12]. The density of metal matrix syntactic foams can be as low as 1 g/cm^3, whereas the densities of commonly fabricated polymer matrix syntactic foams (PMSFs) are in the range of 0.4–0.8 g/cm^3. Hollow glass microballoons (HGM), fly ash cenospheres, and carbon and polymer hollow spheres are widely used as fillers in syntactic foams [2, 11–13]. Interest in developing high performance syntactic foams has resulted in development of hollow particles of ceramics such as SiC [14, 15] and Al_2O_3 [16]. CTE of hollow glass microballoon (HGM)/vinyl ester syntactic foams was found to be 60.4% lower than that of the matrix resin. In comparison, vinyl ester matrix syntactic foam containing SiC hollow spheres has CTE up to 79.3% lower in comparison to the matrix resin [14]. Thus, with the development of the ceramic hollow spheres, properties of syntactic foam beyond the commonly used HGM can be obtained.

Elastomeric matrices have not been commonly used in fabricating syntactic foams and only a few studies are available on polyurethane matrix syntactic foams containing glass hollow particles [17, 18]. Polyurethanes are commonly used in automotive industries as coatings, plastic components, and seat cushion foam [19]. This makes it necessary to understand the strain rate-dependent properties as high strain rates are encountered during an automobile crash. These polymers are also used as rocket motor liners for fastening the composite pellet grains within the motor [20]. In particular, to secure hydroxyl-terminated polybutadiene based composite solid propellants in the rocket motor, butadiene and isocyanate

Table 1: Existing studies on polyurethane/hollow glass microballoon syntactic foams.

Reference	Syntactic foam	Results
[17]	Polyurethane foam filled with HGM	Addition of 15% sepiolite nanofibers and 10% HGM resulted in 240% and 300% increase in the tensile and compressive strength of rigid polyurethane foam
[18]	Polyurethane foam filled with HGM	90 kg/m^3 density foam showed 12% increase in compressive modulus and 10% increase in the compressive strength with addition of 1 wt.% of HGM
[30]	Polyurethane foam filled with HGM (9.5 wt.%)	Isonate CPR-16 formulation: addition of HGM resulted in 45% increase in the compressive strength, with very little increase in the composite density.
[31]	Polyurethane foam filled with HGM (0–40 vol.%)	Flexural modulus increases by 80% with addition of 10% HGM.
[32]	Polyurethane foam filled with silane treated HGM (0–20 wt.%)	50% increase in compressive modulus was observed with addition of 10 wt.% of HGM.
[33]	Polyurethane resin filled with HGM (50 vol.%)	The polyurethane foam showed strain rate sensitivity and the collapse stress increased by 238% at a strain rate of 1185 s^{-1} in comparison to quasistatic compression.

based polyurethanes are used as the liner materials [20]. They are also used as thermal insulation in liquid fuel tanks in spacecraft launch vehicles [21, 22]. Another application for polyurethanes and their foams is in the biomedical field where they are used as bone scaffolds and models for cancellous bones due to their biocompatibility and possessing identical mechanical properties to bones [23, 24].

The existing literature on polyurethane matrix syntactic foams with HGM fillers is summarized in Table 1. Most of these studies have utilized polyurethane foam as the matrix materials and filled HGMs for mechanical property improvement. The gas filled foams are known to have very low mechanical properties. There is lack of results on utilizing the polyurethane resin as a solid matrix medium reinforced with hollow spheres. In the current study, polyurethane matrix syntactic foam reinforced with hollow alumina spheres is fabricated and characterized for quasistatic and high strain rate compressive properties.

2. Materials and Methods

The polyurethane resin and syntactic foam were fabricated by Deep Springs Technologies, Toledo, OH. The polyurethane potting system was a two-part polybutadiene based polyurethane with an isocyanate (30211/40008 Urethane Potting System, Potting Solutions LLC) mixed by weight 100 : 18.4 ratio. The polyurethane resin density was measured to be 1.49 ± 0.02 g/cm^3.

The syntactic foams were prepared with the polyurethane resin as the matrix and hollow alumina spheres ($Al_2O_{3\text{-HP}}$) as the filler. The hollow alumina spheres are formed by a deposition technique followed by inert atmosphere sintering at 1650°C. A sacrificial polymer precursor is used to deposit the Al_2O_3 nano pellets over its surface and is followed by sintering process, where the polymer melts away and hollow Al_2O_3 spheres are formed. The average diameter and wall thickness of spheres were 3 mm and 146 μm, respectively, and the particles were treated with a silane adhesion promoter (Xiameter OFS-6020) prior to potting. The nominal $Al_2O_{3\text{-HP}}$ true density was 0.55 g/cc. The density of synthesized syntactic foam was measured to be 1.13 ± 0.024 g/cm^3.

The syntactic foam and the matrix resin were tested under compression at a wide range of quasistatic and high strain rates. Cylindrical specimens of 10 mm diameter and 10 mm thickness were tested at two different quasistatic strain rates of 0.001 s^{-1} and 0.01 s^{-1} using an Instron 4469 electromechanical test machine fitted with a 50 kN load cell. The load and displacement data were recorded using Bluehill software. At least five specimens were used for compression testing of each material. The high strain rate properties were investigated using an in-house developed split-Hopkinson pressure bar (SHPB) setup. The basic theory and the related physics of SHPB can be found in the published literature [25–27]. The SHPB consists of two long slender aluminum bars (Young's modulus, density, and sound wave velocity of 70 GPa, 2700 kg/m^3, and 5092 m/s, resp.) with the specimen sandwiched between them. The time dependent strain rate $\dot{\varepsilon}(t)$, stress $\sigma(t)$, and strain $\varepsilon(t)$ are calculated by

$$\dot{\varepsilon}(t) = \frac{2c_b\varepsilon_r(t)}{l_0},$$
$$\sigma(t) = \frac{AE\varepsilon_t(t)}{A_0}, \quad (1)$$
$$\varepsilon(t) = \int_0^t \dot{\varepsilon}(t)\,dt,$$

where, c_b is the velocity of sound waves in the bar; $\varepsilon_r(t)$ and $\varepsilon_t(t)$ are the reflected and transmitted axial strain pulses as a function of time, respectively, A and E represent the cross-sectional area and the Young's modulus of the bar material, respectively; and A_0 and l_0 are the cross-sectional area and the length of the test specimen, respectively. The stresses at the front and the back surface of the specimen are evaluated using the incident, reflected, and the transmitted strains using

$$\sigma_{\text{front}} = E\left(\varepsilon_i(t) + \varepsilon_r(t)\right),$$
$$\sigma_{\text{back}} = E\varepsilon_t(t), \quad (2)$$

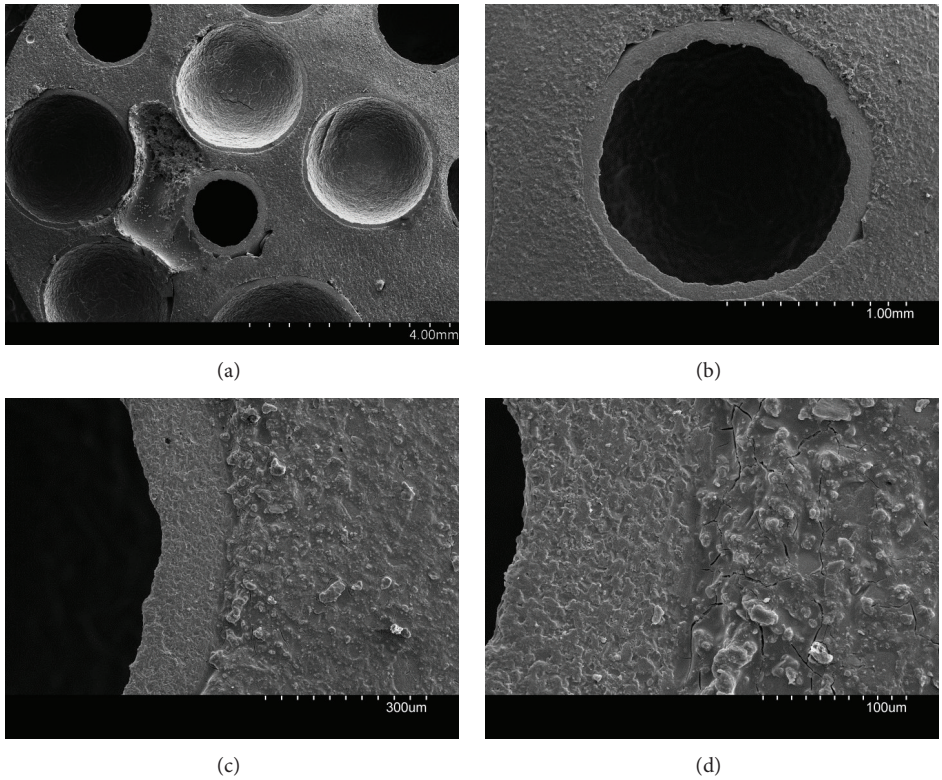

(a) (b) (c) (d)

FIGURE 1: (a) The microstructure of the polyurethane/$Al_2O_{3\text{-HP}}$ syntactic foam: (b), (c), and (d) show the interface between an Al_2O_3 hollow particle and the matrix resin at successively increasing magnifications.

where $\varepsilon_i(t)$ is the incident axial strain pulse. The high strain rate result from the SHPB testing is valid only in the case of dynamic equilibrium, that is, when the stresses at the front and back surfaces of the specimen are comparable [28].

Optical photography of the initial and post test specimens was conducted using a Nikon D7000 DSLR camera equipped with an AF-S VR Micro-Nikkor 105 mm f/2.8G IF-ED macro lens. A Hitachi S-3400N (Hitachi America Ltd., Tarrytown, NY) scanning electron microscope (SEM) was used to observe the specimens before and after testing. The SEM is equipped with secondary electron (SE) and back-scattered electron (BSE) detectors. The specimens were sputter coated with gold before the SEM observation using Leica EM SCD050 (Leica Microsystems Inc., Buffalo Grove, IL).

3. Results and Discussion

The structure of the polyurethane/$Al_2O_{3\text{-HP}}$ syntactic foam is shown in Figure 1(a). Alumina spheres are distributed uniformly in the polyurethane matrix material. The particle-matrix interface is continuous as observed in Figures 1(b) and 1(c). The micrographs of an alumina particle are shown in Figure 2. It is observed that the particle surface has a high degree of roughness and also some porosity. These features are helpful in promoting bonding with the matrix resin. In previous studies on syntactic foams, ceramic hollow spheres of SiC and Al_2O_3 were also observed to have rough surface and porous structure [14, 29]. It is further observed in Figure 1(d) that some cracks exist in the matrix very close to the particle-matrix interface. A large difference in the stiffness of the matrix and particle material causes these cracks to form during sample preparation for microscopy. These cracks are not a microstructure feature in the bulk syntactic foam slab.

A set of representative compressive stress-strain curves of the polyurethane resin at the quasistatic strain rates of $0.001\,s^{-1}$ and $0.01\,s^{-1}$ are plotted in Figure 3. The stress-strain curves of the polyurethane resin under quasistatic compression show a nonlinear behavior. Such resins have a high degree of viscoelasticity. The specimen fractures when the stress reaches the maximum value at the peak of the stress-strain curve. The polyurethane resin shows strain rate sensitivity under quasistatic compression testing conditions, as observed in Figure 3. Although the initial trend of the stress-stain curve is the same, the specimens show considerably higher strength and failure strain at the higher strain rate. The compressive strength and failure strain at $0.001\,s^{-1}$ strain rate are measured to be 9.3 ± 1.5 MPa and $58 \pm 2.0\%$, respectively. In comparison, the strength and failure strain at $0.01\,s^{-1}$ strain rate are found to be 15.2 ± 3.6 MPa and $68 \pm 1.8\%$, respectively. The compressive strength increased by 63.4% and the failure strain increased by 17.2% as the strain rate was increased by an order of magnitude.

The strain signals obtained from the SHPB for the polyurethane resin tested at a strain rate of $5800\,s^{-1}$ are shown in Figure 4(a). The strain rate, stress, and strain are

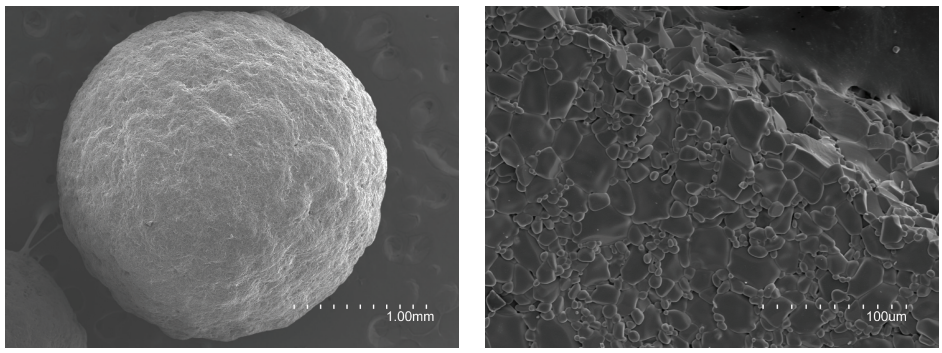

(a) (b)

Figure 2: (a) A single alumina particle of the type used in syntactic foams and (b) close up of the particle surface showing a high degree of surface roughness.

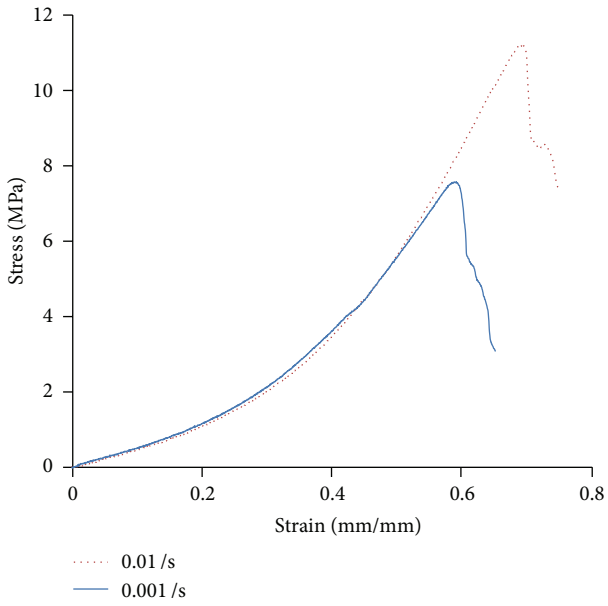

Figure 3: The quasistatic compressive response of the polyurethane resin. Data for one specimen is presented at two different strain rates for comparison.

evaluated from the strain signals using (1) and are shown in Figure 4(b). To obtain valid results from the high strain rate testing, the stress equilibrium in the specimen needs to be attained; that is, the stress on the front and the back surfaces of the specimen should be in close agreement. Figure 4(c) shows close matching in the stress at the two faces of the specimen and validates the test. Similar calculation is conducted for each specimen. The stress-strain curves evaluated from the high strain rate testing of the resin are shown in Figure 5. The general behavior of these curves is similar to the quasistatic compression curves. Note that the y-axis scale is different in Figures 3 and 5 because the specimens demonstrate considerably high strength at high strain rates. It can also be noted in Figure 5 that higher strain rate leads to higher strength in the specimens. All specimens are observed to fracture under the applied loading conditions. The peak stress for the quasistatic and the high strain rates are plotted as a function of the strain rates (on the log scale) and are shown in Figure 6. The peak stress under high strain rate testing for the resin is considerably higher (2–6 times higher for strain rates of 4600–6600 s^{-1}) when compared to quasistatic compression. From Figure 6, it could be observed that two trends emerge from the variation of peak stress with respect to strain rates and that the two trends intersect at a strain rate of 5600 s^{-1}. These observations about the neat resin will be useful in understanding the behavior of syntactic foams.

The stress-strain response of the polyurethane/$Al_2O_{3\text{-HP}}$ syntactic foam is shown in Figure 7. The general trend of the stress-strain curves of the polyurethane syntactic foam is different than that of the polyurethane resin. The stress increases linearly with the strain in the initial elastic region. After the yield point, the specimen deforms plastically before it fractures. The transformation of stress-strain curve from the polyurethane resin to its syntactic foam composite can be attributed to the addition of rigid Al_2O_3 spheres into the viscoelastic polyurethane matrix. Rigid Al_2O_3 particles are load-bearing elements in the syntactic foam microstructure. These particles reduce the overall elasticity of the material. Peaks observed in the stress-strain curve can be attributed to successive failure of the Al_2O_3 spheres as the compressive strain increases. In comparison to the quasistatic testing, the high strain rate results show higher stress values at comparable strain. The yield strength of the polyurethane syntactic foam is specified by the 0.2% offset method and is plotted as a function of the strain rate (on a logarithmic scale) in Figure 8. The yield strength of the polyurethane syntactic foam shows a trend in the strain rate sensitivity that is similar to the matrix resin. It can be expressed as a bilinear relation and the intersection point is observed at a strain rate of 800 s^{-1}.

It should be noted that the polyurethane syntactic foams show quasistatic compressive failure strain in the range of 60–70%. Since there is a considerable difference in the shape of the stress-strain graphs of neat resin and syntactic foams, the energy absorbed up to 10% strain is calculated for comparison and plotted as a function of the strain rate in Figure 9, which

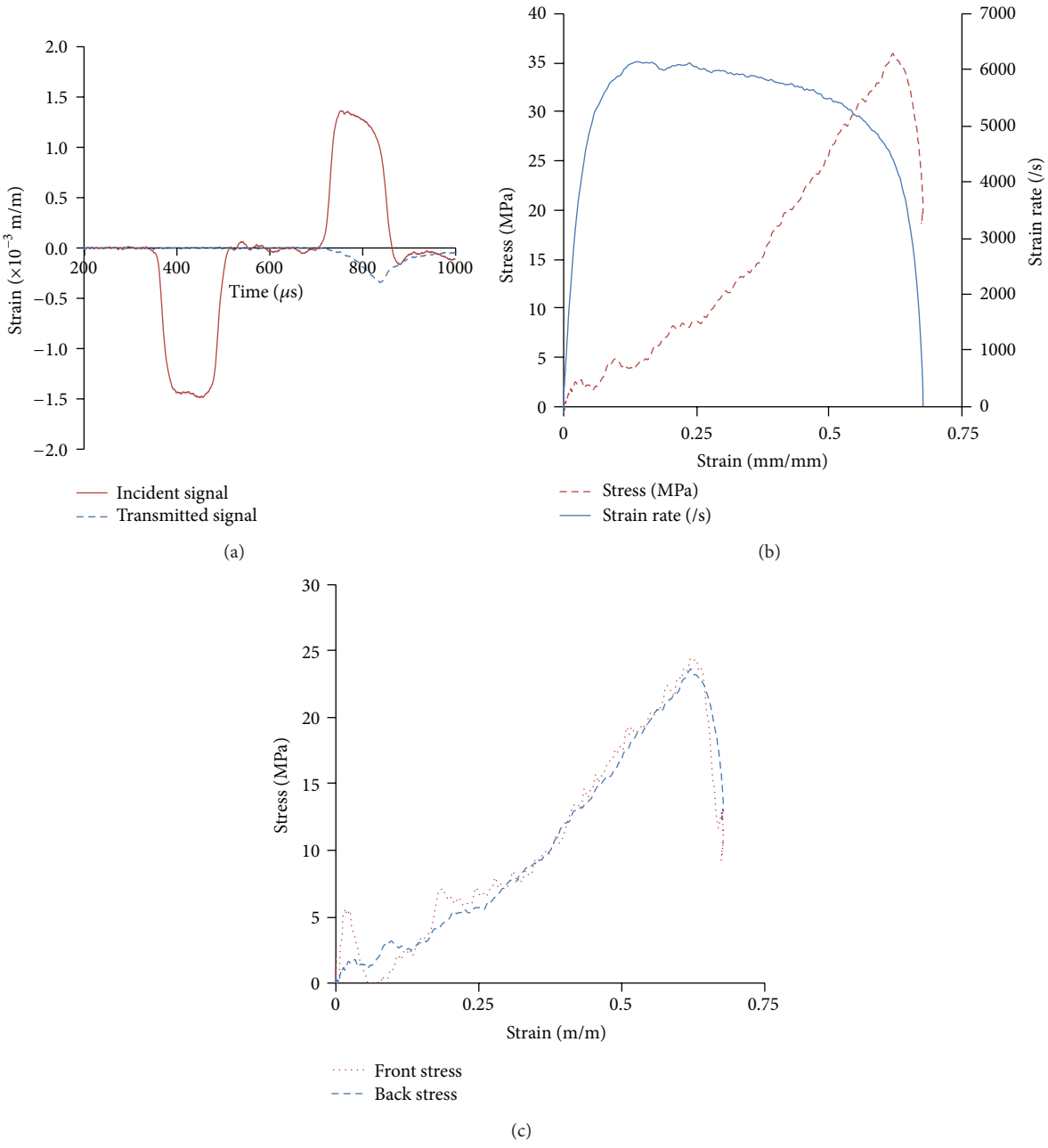

FIGURE 4: (a) Strain signals obtained from the high strain rate testing of the neat resin at a strain rate of 5800 s^{-1}, (b) stress-strain and strain rate-strain plots evaluated from the strain signals, and (c) confirmation of stress equilibrium.

mainly includes elastic energy. The energy absorption of the foam specimens is considerably higher in comparison to the neat resin. In the quasistatic range, the energy absorbed by the foam is 3-4 times the neat resin values. The higher energy absorption in the foam specimens can be attributed to the $Al_2O_{3\text{-HP}}$. The failure of $Al_2O_{3\text{-HP}}$ results in increase in cumulative energy absorption at 10% strain. This type of behavior can be utilized in energy absorbing crash structures in automotive and marine industry, where understanding the energy absorption characteristics with respect to strain rate is important.

Two points are marked as A and B in the quasistatic compressive stress-strain graph of syntactic foam Figure 7(a). The failure of a representative syntactic foam specimen corresponding to these points is shown in Figure 10. It is observed in Figure 10(a) that the initial specimen failure starts as a shear crack across the entire specimen. This point is marked as point "A" in Figure 7(a). $Al_2O_{3\text{-HP}}$ also starts to fracture at point A. Continued compression results in complete crushing of particles and fragmentation of the specimen as observed in Figure 10(b), which represents the final failure of the specimen at the end of the densification region, marked as

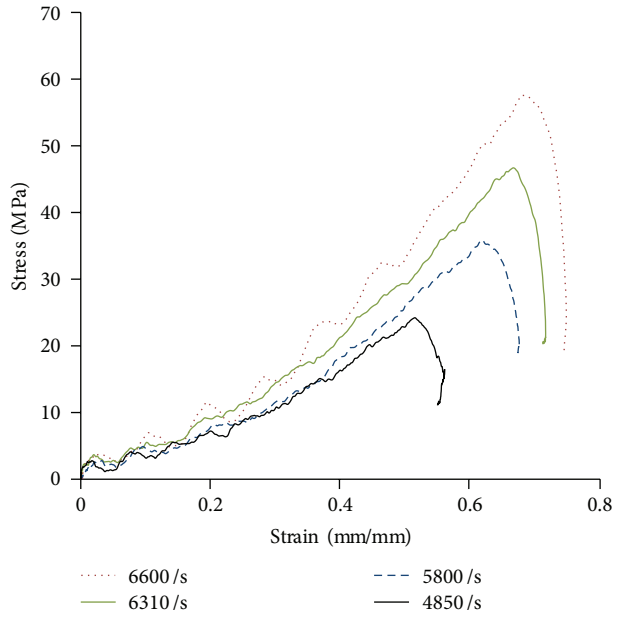

FIGURE 5: The high strain rate compressive response of the polyurethane resin.

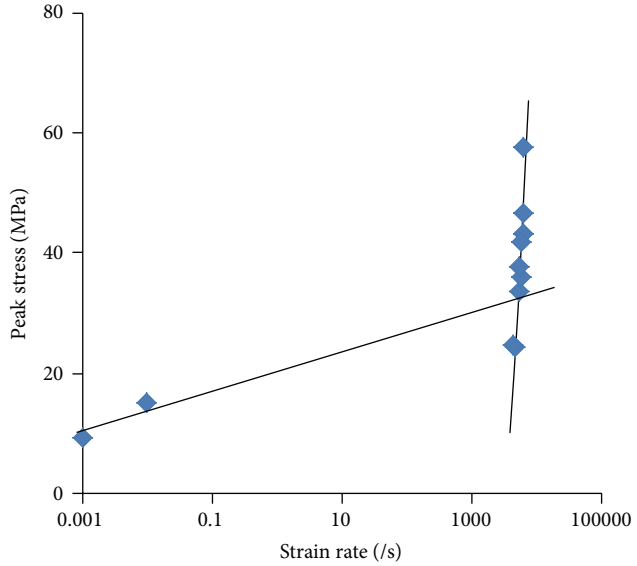

FIGURE 6: The peak stress versus strain rate at logarithm scale for the polyurethane resin. Diamonds represent experimental data points and solid lines represent trend lines.

"B" in Figure 7(a). These features can be compared to that of a specimen that was tested at 1430 s^{-1} strain rate, shown in Figure 11. This specimen shows failure due to shear cracking. The specimen has not been completely crushed because the strain encountered in the high strain rate testing is smaller compared to the strain to which the quasistatic specimens were subjected. $Al_2O_{3\text{-HP}}$ present in this specimen shows signs of crushing. The high strain rate compressive failure is further observed through SEM on a specimen that was subjected to strain rate of 1670 s^{-1}. The arrows marked in Figure 12(a) indicate the compression direction. Micrographs show failure of the $Al_2O_{3\text{-HP}}$ in Figures 12(b), 12(c), and 12(d). It can be observed in these micrographs that the failed hollow spheres are adhering to the matrix resin, indicating a strong particle-matrix interface and effective load transfer from the matrix to the particle.

4. Conclusions

Polyurethane resin and polyurethane/$Al_2O_{3\text{-HP}}$ syntactic foams are studied for compressive properties under quasistatic and high strain rates. The high strain rate compression testing is conducted using a split-Hopkinson pressure bar. The results from the present study can be summarized as follows.

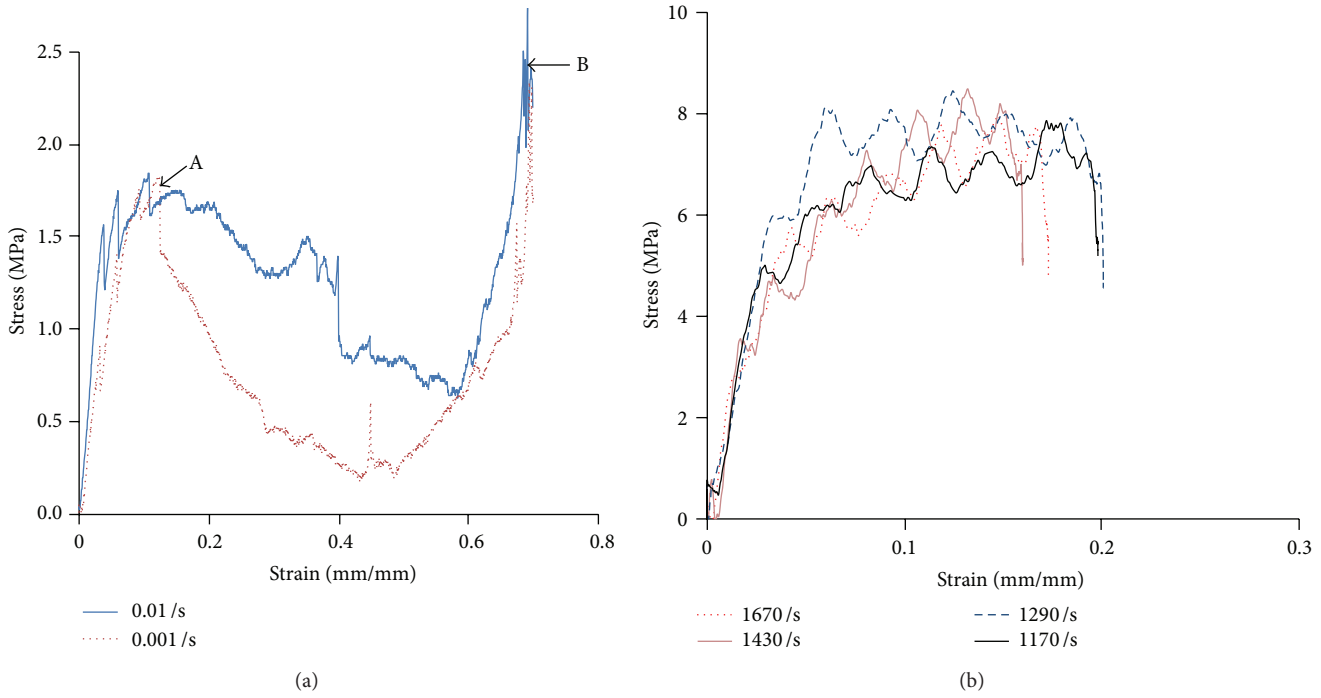

FIGURE 7: The (a) quasistatic and (b) high strain rate responses of the polyurethane/$Al_2O_{3\text{-HP}}$ syntactic foam.

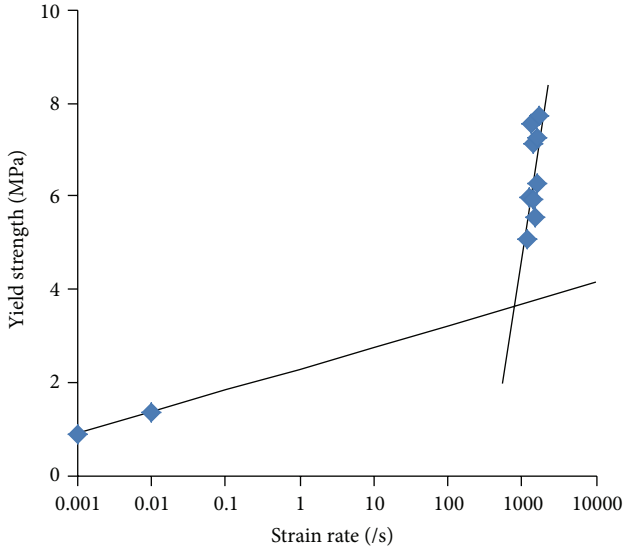

FIGURE 8: The yield strength versus strain rate of the polyurethane/$Al_2O_{3\text{-HP}}$ syntactic foam. Diamonds represent experimental data points and solid lines represent trend lines.

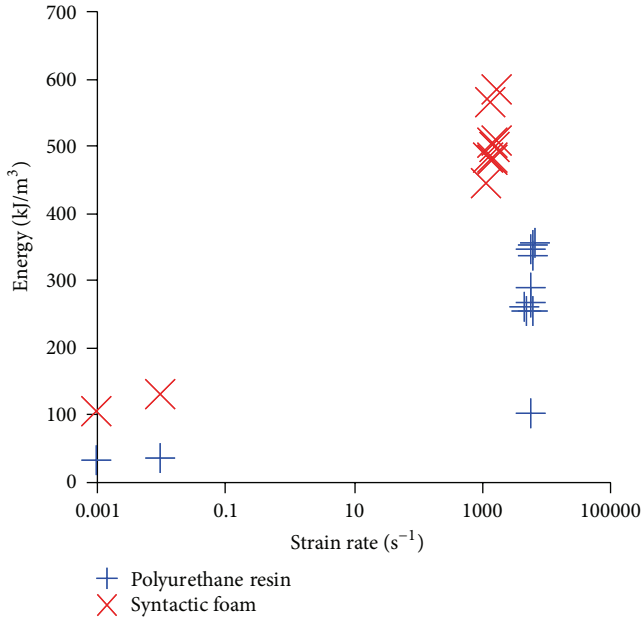

FIGURE 9: Plot of energy absorbed up to 10% strain with respect to the strain rate for neat polyurethane resin and polyurethane/$Al_2O_{3\text{-HP}}$ syntactic foam.

(i) The polyurethane resin shows a viscoelastic quasistatic stress-strain response. Addition of $Al_2O_{3\text{-HP}}$ changes the stress-strain trend of the material. Syntactic foams are observed to have an initial linear elastic region followed by a plastic region that corresponds to particle crushing.

(ii) Both the polyurethane resin and its syntactic foam show strain rate sensitivity in compressive strength. Two different trends were observed in the plot of compressive strength as a function of the strain rate (on the logarithmic scale) for the quasistatic and the high strain rate regimes.

(iii) The energy absorbed up to 10% strain in the quasistatic regime is 400% higher for the syntactic foam in comparison to the neat resin.

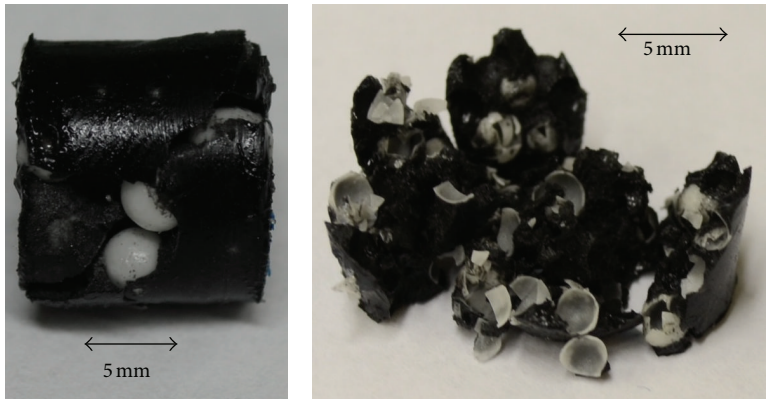

(a) (b)

Figure 10: Fracture features of polyurethane/$Al_2O_{3\text{-HP}}$ syntactic foam specimens tested under compression at strain rates of 0.01 s^{-1}. Parts (a) and (b) correspond to the points A and B, respectively, marked in Figure 7(a).

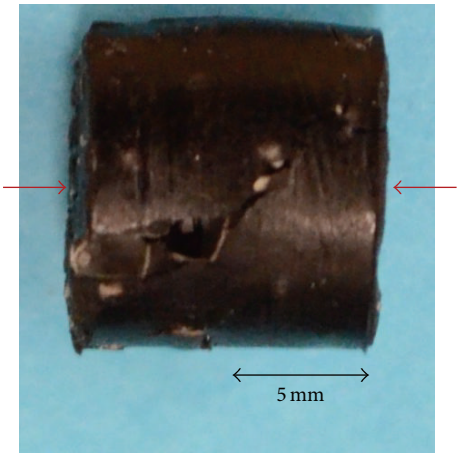

Figure 11: Fracture features of polyurethane/$Al_2O_{3\text{-HP}}$ syntactic foam specimens tested under compression at strain rates of 1430 s^{-1}.

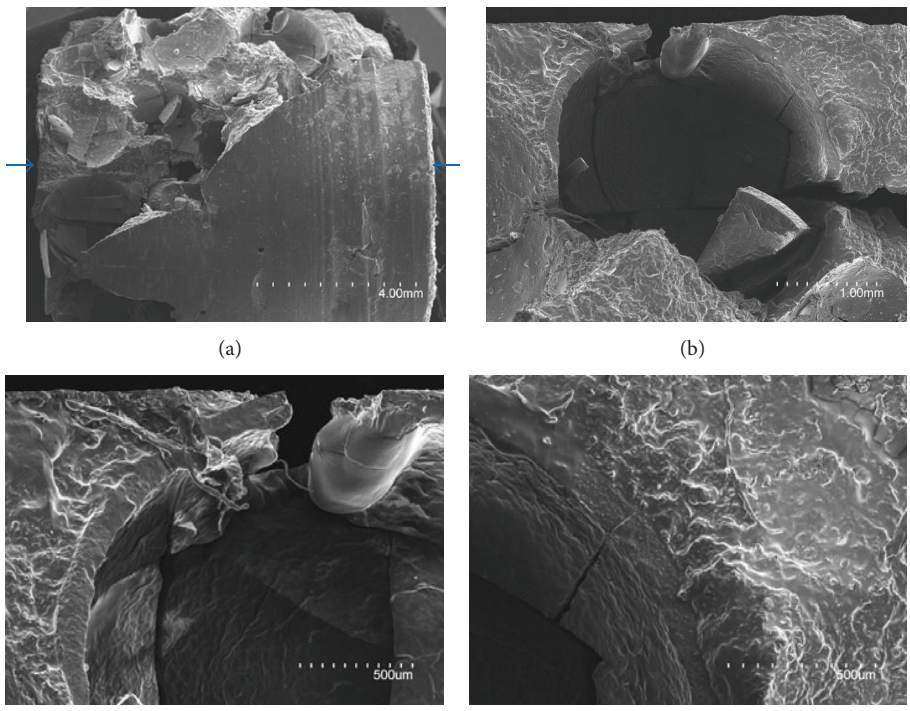

(a) (b)

(c) (d)

Figure 12: SEM images of a polyurethane/Al_2O_3 syntactic foam specimen tested at a strain rate of 1670 s^{-1} showing the (a) specimen shear failure and (b), (c), and (d) failure of a hollow particle.

(iv) The failure of the syntactic foam occurs through shearing of matrix resin, followed by failure of the hollow particles. The interface between the $Al_2O_{3\text{-HP}}$ and the matrix resin on the failed specimens was intact, indicating effective load transfer between the matrix and the hollow particle.

Conflict of Interests

The authors declare no conflict of interests.

Acknowledgments

Portions of the research reported in this paper were performed in connection with U.S. Army Research Laboratory contract W911NF-10-2-0084 with DST and through the Office of Naval Research Grant N00014-10-1-0988 to NYU-Poly. The authors thank Steven E. Zeltmann for help in the paper preparation. The views and conclusions contained in this presentation are those of the authors and should not be interpreted as presenting the official policies or position, either expressed or implied, of the ARL or the U.S. Government unless so designated by other authorized documents. Citation of manufacturers' or trade names does not constitute an official endorsement or approval of the use notwithstanding any copyright notation hereon.

References

[1] F. A. Shutov, "Syntactic polymer foams," in *Chromatography/Foams/Copolymers*, pp. 63–123, Springer, Berlin, Germany, 1986.

[2] N. Gupta, D. Pinisetty, and V. Shunmugasamy, *Reinforced Polymer Matrix Syntactic Foams Effect of Nano and Micro-Scale Reinforcement*, Springer, New York, NY, USA, 2013.

[3] M. Porfiri and N. Gupta, "Effect of volume fraction and wall thickness on the elastic properties of hollow particle filled composites," *Composites Part B: Engineering*, vol. 40, no. 2, pp. 166–173, 2009.

[4] P. Bunn and J. T. Mottram, "Manufacture and compression properties of syntactic foams," *Composites*, vol. 24, no. 7, pp. 565–571, 1993.

[5] V. S. Shabde, K. A. Hoo, and G. M. Gladysz, "Experimental determination of the thermal conductivity of three-phase syntactic foams," *Journal of Materials Science*, vol. 41, no. 13, pp. 4061–4073, 2006.

[6] V. C. Shunmugasamy, D. Pinisetty, and N. Gupta, "Thermal expansion behavior of hollow glass particle/vinyl ester composites," *Journal of Materials Science*, vol. 47, no. 14, pp. 5596–5604, 2012.

[7] N. Gupta and D. Pinisetty, "A review of thermal conductivity of polymer matrix syntactic foams—effect of hollow particle wall thickness and volume fraction," *JOM*, vol. 65, no. 2, pp. 234–245, 2013.

[8] B. Zhu, J. Ma, J. Wang, J. Wu, and D. Peng, "Thermal, dielectric and compressive properties of hollow glass microsphere filled epoxy-matrix composites," *Journal of Reinforced Plastics and Composites*, vol. 31, no. 19, pp. 1311–1326, 2012.

[9] B. L. Zhu, H. Zheng, J. Wang, J. Ma, J. Wu, and R. Wu, "Tailoring of thermal and dielectric properties of LDPE-matrix composites by the volume fraction, density, and surface modification of hollow glass microsphere filler," *Composites B: Engineering*, vol. 58, pp. 91–102, 2014.

[10] V. C. Shunmugasamy, D. Pinisetty, and N. Gupta, "Electrical properties of hollow glass particle filled vinyl ester matrix syntactic foams," *Journal of Materials Science*, vol. 49, no. 1, pp. 180–190, 2014.

[11] B. John and C. P. R. Nair, *Update on Syntactic Foams*, iSmithers Rapra, Shropshire, UK, 2010.

[12] N. Gupta and P. K. Rohatgi, Eds., *Metal Matrix Syntactic Foams: Processing, Microstructure, Properties and Applications*, DEStech Publications, Lancaster, Pa, USA, 2014.

[13] M. Labella, S. E. Zeltmann, V. C. Shunmugasamy, N. Gupta, and P. K. Rohatgi, "Mechanical and thermal properties of fly ash/vinyl ester syntactic foams," *Fuel*, vol. 121, pp. 240–249, 2014.

[14] M. Labella, V. C. Shunmugasamy, O. M. Strbik, and N. Gupta, "Compressive and thermal characterization of syntactic foams containing hollow silicon carbide particles with porous shell," *Journal of Applied Polymer Science*, vol. 131, no. 17, pp. 1–5, 2014.

[15] D. D. Luong, O. M. Strbik III, V. H. Hammond, N. Gupta, and K. Cho, "Development of high performance lightweight aluminum alloy/SiC hollow sphere syntactic foams and compressive characterization at quasi-static and high strain rates," *Journal of Alloys and Compounds*, vol. 550, pp. 412–422, 2013.

[16] L. Licitra, D. D. Luong, O. M. Strbik III, and N. Gupta, "Dynamic properties of alumina hollow particle filled aluminum alloy A356 matrix syntactic foams," *Materials & Design*, 2014.

[17] F. Wang, Q. Tang, X. Duan et al., "Effect of modified sepiolite nanofibers and hollow glass microspheres on performance of rigid polyurethane foams composite materials," *Nanoscience and Nanotechnology Letters*, vol. 6, no. 6, pp. 524–531, 2014.

[18] V. Yakushin, L. Bel'kova, and I. Sevastyanova, "Properties of rigid polyurethane foams filled with glass microspheres," *Mechanics of Composite Materials*, vol. 48, no. 5, pp. 579–586, 2012.

[19] R. Deng, P. Davies, and A. K. Bajaj, "Flexible polyurethane foam modelling and identification of viscoelastic parameters for automotive seating applications," *Journal of Sound and Vibration*, vol. 262, no. 3, pp. 391–417, 2003.

[20] S. Benli, Ü. Yilmazer, F. Pekel, and S. Özkar, "Effect of fillers on thermal and mechanical properties of polyurethane elastomer," *Journal of Applied Polymer Science*, vol. 68, no. 7, pp. 1057–1065, 1998.

[21] X. B. Zhang, J. Y. Chen, Z. H. Gan et al., "Experimental study of moisture uptake of polyurethane foam subjected to a heat sink below 30 K," *Cryogenics*, vol. 59, pp. 1–6, 2014.

[22] A. Demharter, "Polyurethane rigid foam, a proven thermal insulating material for applications between +130°C and −196°C," *Cryogenics*, vol. 38, no. 1, pp. 113–117, 1998.

[23] N. B. Shelke, R. K. Nagarale, and S. G. Kumbar, "Polyurethanes," in *Natural and Synthetic Biomedical Polymers*, S. G. Kumbar, C. T. Laurencin, and M. Deng, Eds., pp. 123–144, Elsevier, Oxford, UK, 2014.

[24] P. S. D. Patel, D. E. T. Shepherd, and D. W. L. Hukins, "Compressive properties of commercially available polyurethane foams as mechanical models for osteoporotic human cancellous bone," *BMC Musculoskeletal Disorders*, vol. 9, article 137, 2008.

[25] N. Gupta, D. D. Luong, and P. K. Rohatgi, "A method for intermediate strain rate compression testing and study of compressive failure mechanism of Mg-Al-Zn alloy," *Journal of Applied Physics*, vol. 109, no. 10, Article ID 103512, 2011.

[26] D. D. Luong, N. Gupta, A. Daoud, and P. K. Rohatgi, "High strain rate compressive characterization of aluminum alloy/fly ash cenosphere composites," *JOM: Journal of Minerals, Metals and the Materials Society*, vol. 63, no. 2, pp. 53–56, 2011.

[27] W. Chen and B. Song, "Conventional Kolsky bars," in *Split Hopkinson (Kolsky) Bar*, pp. 1–35, Springer, New York, NY, USA, 2011.

[28] B. Song and W. Chen, "Dynamic stress equilibration in split Hopkinson pressure bar tests on soft materials," *Experimental Mechanics*, vol. 44, no. 3, pp. 300–312, 2004.

[29] V. Shunmugasamy, S. Zeltmann, N. Gupta, and O. Strbik III, "Compressive characterization of single porous SiC hollow particles," *JOM: Jounal of Minerals, Metals and Materials Society*, vol. 66, no. 6, pp. 892–897, 2014.

[30] E. Barber, J. Nelson, and W. Beck, "Improving properties in rigid urethane foams using glass bubbles," *Journal of Cellular Plastics*, vol. 13, no. 6, pp. 383–392, 1977.

[31] J. A. Hagarman, J. P. Cunnion, and B. W. Sands, "Formulation and physical properties of polyurethane foam incorporating hollow microspheres," *Journal of Cellular Plastics*, vol. 21, no. 6, pp. 406–408, 1985.

[32] X.-C. Bian, J.-H. Tang, and Z.-M. Li, "Flame retardancy of hollow glass microsphere/rigid polyurethane foams in the presence of expandable graphite," *Journal of Applied Polymer Science*, vol. 109, no. 3, pp. 1935–1943, 2008.

[33] A. Pellegrino, V. L. Tagarielli, R. Gerlach, and N. Petrinic, "The mechanical response of a syntactic polyurethane foam at low and high rates of strain," *International Journal of Impact Engineering*, vol. 75, pp. 214–221, 2015.